A Discrete Model for Force-Based Elasticity and Plasticity

Ioannis Dassios[1*], Georgios Tzounas[2], Federico Milano[1], Andrey Jivkov[3]

[1]University College Dublin, Ireland

[2]ETH Zürich, Switzerland

[3]University of Manchester, UK

[*]Corresponding author

Abstract: The article presents a mathematical model that simulates the elastic and plastic behaviour of discrete systems representing isotropic materials. The systems consist of one lattice of nodes connected by edges and a second lattice with nodes placed at the centres of the existing edges. The derivation is based on the assumption that the kinematics of the second lattice is induced by the kinematics of the first, and uses stored energies in edges of both lattices to derive a edge forces in the first lattice. This leads to a non-linear system of algebraic equations describing elasticity and plasticity in lattices. A numerical solution to the non-linear system is proposed by providing a matrix formulation necessary for software implementation. An illustrative example is given to justify the formulation and demonstrate the system behaviour.

Keywords : lattice model, elasticity, plasticity, energy, non-linear system.

1 Introduction

The modelling of solids with lattices has been initially developed for failure analysis of quasi-brittle materials, such as concretes and rocks [1], [2]. This has been dictated by the need to represent the generation of micro-cracks and their coalescence into macro-cracks leading to material failure in a computationally efficient manner. The emergence of a micro-crack, i.e., of two internal surfaces, dissipates stored/elastic energy and from a mathematical perspective is a topological evolution of the analysed material domain. Describing this process is outside the remit of the classical continuum mechanics which is a thermodynamic *bulk* theory. A widely used approach to overcome this limitation using existing numerical methods for continuum mechanics problems, such as the finite element method, is the cohesive zone modelling [3]. This requires insertion of special cohesive elements between standard finite elements that allow for generation of new surfaces but make the analysis both mesh size dependent and computationally demanding. In contrast, lattice modelling is less demanding and particularly suitable for quasi-brittle materials as they are characterised by initial generation of a large population of randomly distributed micro-cracks [4]. Under tension, these materials are elastic-brittle, where energy is dissipated almost entirely by generation of new surfaces. This simplifies the formulation of the lattice behaviour. However, under compression the micro-crack generation

is in competition with local plasticity for dissipating stored energy [5]. The competition between plasticity and surface generation is most pronounced in metallic materials, where energy is dissipated predominantly by plasticity prior to surface generation [6]. The development of lattice models with elastic-plastic material behaviour will be beneficial for failure analysis in such cases.

Lattice models contain nodes connected by edges, i.e., they are mathematical graphs embedded in $\mathbb{R}^2$ or $\mathbb{R}^3$ depending on the required analysis. The models are intended to represent a *continuous* solid by a discrete system. Specifically, the stored energy in any lattice region is required to be equivalent to the stored energy in the corresponding continuum region. This is used to derive a link between the elastic properties of lattice elements, e.g., edge stiffness coefficients, and the macroscopic properties of the material, but such a derivation is challenging for general graphs. For graphs with some regularity, the link can be established exactly. For example, isotropic materials, whose macroscopic behaviour is described by two elastic constants, can be represented by $2D$ graphs based on hexagonal structure, e.g. [7], and by $3D$ graphs based on truncated octahedral structure [8], [9]. Other regular and semi-regular $3D$ graphs can represent materials with cubic elasticity, i.e., whose macroscopic behaviour is described by three elastic constants, but not isotropic elasticity typical for most engineering materials [10]. Nevertheless, lattices are being used to represent failure in materials, albeit not always with exactly calibrated local properties.

A mathematically rigorous treatment of lattices can be achieved when they are analysed as graphs [11], using elements of the discrete exterior calculus (DEC) [12]. However, the standard DEC has been developed for problems involving conservation of scalar quantities, such as energy, mass, and electric charge. In such case, the problem unknown is a discrete scalar field over the nodes (a 0-cochain), e.g., temperature, pressure, concentration, etc. The variation of this field providing fluxes via a constitutive relation is a scalar field over the edges (a 1-cochain), and the conservation/balance is established at nodes. Details of this formulation and its software implementation can be found in [13]. An alternative to DEC for conservation of scalar quantities that respects given discrete structure exactly has been recently developed using Forman's combinatorial differential forms [14]. In contrast, the conservation of linear and angular momenta required for mechanical problems is rather more difficult as the problem unknown is a vector-valued nodal field, namely displacement vectors assigned to each node. One possibility is to work with discrete sharps and flats, similar to the ones suggested in [12], and build a discrete analogue of the continuum mechanics in terms of kinematics, constitutive relations and balance of momenta [15]. While this approach is acceptable, it is still computationally demanding and for large discrete structures the modelling with lattices remains attractive.

In a previous work [16] we have developed a simple representation of plasticity and damage in $3D$ lattices using elements of DEC and attributing the elastic-plastic behaviour to the individual lattice elements (edges). However, it has been recognised that such an approach does not correspond directly to the classical continuum plasticity where plastic flow is independent of the hydrostatic stress component and is controlled by the deviatoric stresses only. In a

subsequent work [17] we have proposed a structure comprising the main graph and a complementary graph that allows for better representation of the internal forces and have analysed its elastic behaviour. The aim of the present work is to build upon the past works and develop a graph-theoretical approach to elasto-plasticity of graphs. In Section 2 we construct a model containing a main graph with nodes and edges and a second graph with nodes placed at the centres of the main edges. The construction represents the initial state of the material. We then consider the kinematics of the second graph to be induced by the kinematics of the main one. Using a force-based approach and the stored energy associated with the bonds in both graphs we arrive at a non-linear system of algebraic equations describing the elasticity and plasticity of the material. In Section 3 we provide a numerical method for the solutions of the non-linear system, a method appropriate for software implementation. Section 4 contains a numerical example based on our theory. We close the paper with the section of conclusions.

2 Model with Calculus on Discrete Manifolds

Consider a lattice $\mathcal{G}$ containing a set of n nodes connected by m edges via the algebraic system:

$$AN = E,$$

where A is the incidence matrix, containing m rows and n columns:

$$A = [a_{ij}]_{i=1,2,...,m}^{j=1,2,...,n} \in \mathbb{R}^{m\times n},$$

with coefficients given by

$$a_{ij} = \begin{cases} 0, & \text{if node } j \text{ is not a node of edge } i \\ 1, & \text{if node } j \text{ is the first node of edge } i \\ -1, & \text{if node } j \text{ is the second node of edge } i \end{cases}$$

In discrete calculus, A is an algebraic representation of both the topology and the co-boundary operator that maps a 0-cochain (a function over the nodes) to a 1-cochain (a function over the edges), see [11]. The nodal coordinates are presented as a discrete vector-valued function over nodes encoded by the matrix

$$N = \begin{bmatrix} N_1 \\ N_2 \\ \vdots \\ N_n \end{bmatrix} \in \mathbb{R}^{n\times 3}, \quad \text{where} \quad N_i = \begin{bmatrix} N_{i1} & N_{i2} & N_{i3} \end{bmatrix} \in \mathbb{R}^{1\times 3}, \quad i = 1, 2, ..., n.$$

The discrete vector-valued function over edges obtained from N by the map A is given by the matrix

$$E = \begin{bmatrix} E_1 \\ E_2 \\ \vdots \\ E_m \end{bmatrix} \in \mathbb{R}^{m\times 3}, \quad \text{where} \quad E_i = \begin{bmatrix} E_{i1} & E_{i2} & E_{i3} \end{bmatrix} \in \mathbb{R}^{1\times 3}, \quad i = 1, 2, ..., m$$

and contains vectors along edges from where the lengths of all edges E_i, i.e. $|E_i|$, $i = 1, 2, ..., m$, are calculated.

Consider now a second lattice $\hat{\mathcal{G}}$ with $\hat{n}$ nodes, placed exactly at the centres of the existing edges, i.e. the number of these nodes is $\hat{n} = m$, and $\hat{m}$ secondary edges connecting secondary nodes corresponding to existing edges with common exiting nodes. The topology of the second lattice is described by an incidence matrix $\hat{A}$, containing $\hat{m}$ rows and $\hat{n} = m$ columns. Its structure depends on the existing lattice, i.e., on A.

The coordinates of the secondary nodes are $\hat{N}_i = \frac{1}{2}(N_j + N_k)$, where i is the index of the secondary node (equal to the index of the primary edge) and j, k are the indices of the primary nodes at the ends of edge i. Let the nodal coordinates of the secondary lattice be represented by a discrete vector-valued function over secondary nodes

$$\hat{N} = \begin{bmatrix} \hat{N}_1 \\ \hat{N}_2 \\ \vdots \\ \hat{N}_{\hat{n}} \end{bmatrix} \in \mathbb{R}^{\hat{n}\times 3}, \quad \text{where} \quad \hat{N}_i = \begin{bmatrix} \hat{N}_{i1} & \hat{N}_{i2} & \hat{N}_{i3} \end{bmatrix} \in \mathbb{R}^{1\times 3}, \quad i = 1, 2, ..., \hat{n}.$$

This is obtained from the coordinates of the existing nodes by

$$\hat{N} = SN$$

where

$$S = [s_{ij}]_{i=1,2,...,m}^{j=1,2,...,n} \in \mathbb{R}^{m\times n}, \quad s_{ij} = \begin{cases} 0, & \text{if node } j \text{ is not a node of edge } i. \\ 0.5, & \text{if node } j \text{ is a node of edge } i. \end{cases}$$

The discrete vector-valued function over secondary edges obtained from $\hat{N}$ by the map $\hat{A}$ is given by the matrix

$$\hat{E} = \begin{bmatrix} \hat{E}_1 \\ \hat{E}_2 \\ \vdots \\ \hat{E}_{\hat{m}} \end{bmatrix} \in \mathbb{R}^{\hat{m}\times 3}, \quad \text{where} \quad \hat{E}_i = \begin{bmatrix} \hat{E}_{i1} & \hat{E}_{i2} & \hat{E}_{i3} \end{bmatrix} \in \mathbb{R}^{1\times 3}, \quad i = 1, 2, ..., \hat{m},$$

and contains vectors along secondary edges from where the lengths of all edges $\hat{E}_i$, i.e. $|\hat{E}_i|$, $i = 1, 2, ..., \hat{m}$ are calculated. The matrix $\hat{A}$, which has $\hat{m}$ rows and $\hat{n} = m$ columns, satisfies the equation:

$$\hat{A}\hat{N} = \hat{E}.$$

When the incidence matrices A, $\hat{A}$ derive from a Voronoi tessellation of space by connecting the centres of cells with common faces with an edge, they are very sparse matrices – very far from full graph based on the two node sets (primary and secondary).

A boundary value problem is formulated by prescribing boundary conditions at the nodes of $\mathcal{G}$. These can be either Neumann, i.e. prescribed external forces, or Dirichlet, i.e. prescribed new coordinates due to nodal displacements. As a result, the geometry of the structure changes, so that the nodes of $\mathcal{G}$ and $\hat{\mathcal{G}}$ attain new coordinates. Let

$$X = \begin{bmatrix} X_1 \\ X_2 \\ \vdots \\ X_n \end{bmatrix} \in \mathbb{R}^{n\times 3}, \quad \text{where} \quad X_i = \begin{bmatrix} X_{i1} & X_{i2} & X_{i3} \end{bmatrix} \in \mathbb{R}^{1\times 3}, \quad i = 1, 2, ..., n.$$

be the new nodal coordinates of $\mathcal{G}$, and

$$\hat{X} = \begin{bmatrix} \hat{X}_1 \\ \hat{X}_2 \\ \vdots \\ \hat{X}_{\hat{n}} \end{bmatrix} \in \mathbb{R}^{\hat{n}\times 3}, \quad \text{where} \quad \hat{X}_i = \begin{bmatrix} \hat{X}_{i1} & \hat{X}_{i2} & \hat{X}_{i3} \end{bmatrix} \in \mathbb{R}^{1\times 3}, \quad i = 1, 2, ..., \hat{n}.$$

be the new nodal coordinates of $\hat{\mathcal{G}}$. We require that

$$\hat{X} = SX,$$

i.e., that the positions of the secondary nodes relative to the existing ones do not change; in other words the deformation of $\hat{\mathcal{G}}$ is consistent with the deformation of $\mathcal{G}$.

The action of A on X provides the matrix

$$Y = \begin{bmatrix} Y_1 \\ Y_2 \\ \vdots \\ Y_m \end{bmatrix} \in \mathbb{R}^{m\times 3}, \quad \text{where} \quad Y_i = \begin{bmatrix} Y_{i1} & Y_{i2} & Y_{i3} \end{bmatrix} \in \mathbb{R}^{1\times 3}, \quad i = 1, 2, ..., m.$$

containing vectors along the existing edges in the deformed state, from where their lengths are readily calculated:

$$AX = Y. \tag{1}$$

The action of $\hat{A}$ on $\hat{X}$ provides the matrix

$$\hat{Y} = \begin{bmatrix} \hat{Y}_1 \\ \hat{Y}_2 \\ \vdots \\ \hat{Y}_{\hat{m}} \end{bmatrix} \in \mathbb{R}^{\hat{m}\times 3}, \quad \text{where} \quad \hat{Y}_i = \begin{bmatrix} \hat{Y}_{i1} & \hat{Y}_{i2} & \hat{Y}_{i3} \end{bmatrix} \in \mathbb{R}^{1\times 3}, \quad i = 1, 2, ..., \hat{m}.$$

containing vectors along the existing edges in the deformed state, from where their lengths are readily calculated:

$$A\hat{X} = \hat{Y}.$$

Solid materials accommodate strain from external loading by reversible (elastic) rearrangement, giving rise to internal stresses, and by dissipating energy via slip (plasticity) or separation (surface generation). In the graph framework, the stress is a vector-valued function over the edges (not a tensor as in continuum mechanics) acting along their current (deformed) orientation. Let $\frac{Y_i}{|Y_i|}$, $i = 1, 2, ..., m$, be the unit vectors along edges of lattice $\mathcal{G}$, where $|Y_i|$, are the new edge lengths. For $\mathcal{G}$, the edge forces F_i, $\forall i = 1, 2, ..., m$, are given by

$$\frac{1}{|F_i|}F_i = \frac{1}{|Y_i|}Y_i, \quad i = 1, 2, ..., m,$$

which can be summarised for the whole $\mathcal{G}$ by

$$F = g(Y)Y, \quad \text{where} \quad g(Y) = \text{diag}\left\{\frac{|F_1|}{|Y_1|}, \frac{|F_2|}{|Y_2|}, \ldots, \frac{|F_m|}{|Y_m|}\right\} \in \mathbb{R}^{m\times m}. \tag{2}$$

Similarly for lattice $\hat{\mathcal{G}}$, the edge forces $\hat{F}_i$, $\forall j = 1, 2, ..., \hat{m}$, are given by

$$\frac{1}{|\hat{F}_j|}\hat{F}_j = \frac{1}{|\hat{Y}_j|}\hat{Y}_j, \quad j = 1, 2, ..., \hat{m}.$$

which can be summarised for the whole $\hat{\mathcal{G}}$ by

$$\hat{F} = g(\hat{Y})\hat{Y}, \quad \text{where} \quad g(\hat{Y}) = \text{diag}\left\{\frac{|\hat{F}_1|}{|\hat{Y}_1|}, \frac{|\hat{F}_2|}{|\hat{Y}_2|}, \ldots, \frac{|\hat{F}_{\hat{m}}|}{|\hat{Y}_{\hat{m}}|}\right\} \in \mathbb{R}^{\hat{m}\times\hat{m}}.$$

For the lattice $\mathcal{G}$, F_i are related to the edge elongations, $|Y_i| - |E_i|$, via a

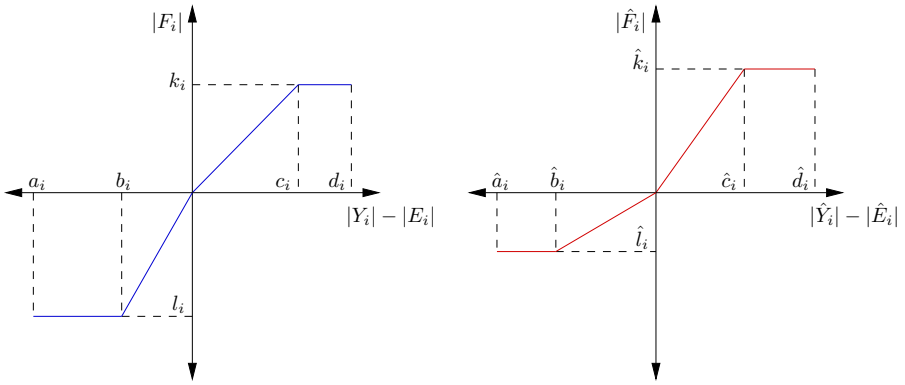

Figure 1: On the left the plot of the non-smooth function that relates $|F_i|$ with $|Y_i| - |E_i|$ of $\mathcal{G}$. On the right the plot of the non-smooth function that relates $|\hat{F}_i|$ with $|\hat{Y}_i| - |\hat{E}_i|$ of $\hat{\mathcal{G}}$.

potentially non-smooth function as illustrated in Fig. 1 (left). Similarly, for the

lattice $\hat{\mathcal{G}}$, $\hat{F}_j$ are related to the edge elongations, $|\hat{Y}_j| - |\hat{E}_j|$, via potentially a non-smooth function as illustrated in Fig. 1 (right).

Upon deformation, the edges of $\mathcal{G}$ and $\hat{\mathcal{G}}$ store energy, U_i, for $i = 1, 2, ..., m$ and $\hat{U}_j$, for $j = 1, 2, ..., \hat{m}$, respectively. These energies are dependent on the length changes $|Y_i| - |E_i|$, $i = 1, 2, ..., m$ and $|\hat{Y}_j| - |\hat{E}_j|$, $j = 1, 2, ..., \hat{m}$, respectively. Taking into account that the deformation of $\hat{\mathcal{G}}$ is induced by $\hat{X} = SX$, it is clear that the system unknowns (nodal coordinates) are associated with the nodes of $\mathcal{G}$ only and correspondingly the system reaction (edge forces) need to be associated with the edges of $\mathcal{G}$ only. To achieve this, we associate the stored energy of the system only with the edges of $\mathcal{G}$, making the total energy of $\mathcal{G}$-edge i equal to the sum of its internal energy, U_i, and half of the energies in the $\hat{\mathcal{G}}$-edges incident with the $\hat{\mathcal{G}}$-node centred at $\mathcal{G}$-edge i. This can be written as $\frac{1}{2}\sum_{j=1}^{\hat{m}} \hat{U}_j$, where the sum is over the $\hat{\mathcal{G}}$-edges incident with the $\hat{\mathcal{G}}$-node. Thus, the gradient of the total energy with respect to the change of edge length, provides the magnitude of the force in the $\mathcal{G}$-edge, i.e. for $|Y_i| - |E_i|$ we have

$$\frac{1}{2}|F_i|\big(|Y_i| - |E_i|\big) = U_i + \frac{1}{2}\sum_{j=1}^{\hat{m}} \hat{U}_j, \quad i = 1, 2, ..., m. \tag{3}$$

Let

$$B = \begin{bmatrix} B_1 \\ B_2 \\ \vdots \\ B_n \end{bmatrix} \in \mathbb{R}^{n\times 3}, \quad \text{where} \quad B_i = \begin{bmatrix} B_{i1} & B_{i2} & B_{i3} \end{bmatrix} \in \mathbb{R}^{1\times 3}, \quad i = 1, 2, ..., n,$$

be the external forces at the nodes of $\mathcal{G}$, either provided as Neumann boundary conditions, or arising as reactions to essential boundary conditions, and let

$$\hat{B} = \begin{bmatrix} \hat{B}_1 \\ \hat{B}_2 \\ \vdots \\ \hat{B}_{\hat{n}} \end{bmatrix} \in \mathbb{R}^{\hat{n}\times 3}, \quad \text{where} \quad \hat{B}_i = \begin{bmatrix} \hat{B}_{i1} & \hat{B}_{i2} & \hat{B}_{i3} \end{bmatrix} \in \mathbb{R}^{1\times 3}, \quad i = 1, 2, ..., \hat{n}.$$

be the external forces at the nodes of $\hat{\mathcal{G}}$.

Since the balance of angular momentum is automatically fulfilled at all nodes, the equilibrium of the system with the boundary conditions is ensured by the balance of linear momentum at all nodes. This is given by

$$A^\intercal F = B, \tag{4}$$

where $A^\intercal \in \mathbb{R}^{n\times m}$ is the transpose of the incidence matrix A, a boundary operator on edges of $\mathcal{G}$. By substituting (2) into (4), we get

$$A^\intercal g(|Y|)Y = B,$$

which incorporates the contribution of $\hat{\mathcal{G}}$. By substituting (1) into this non-linear system, we arrive at the general description of the system elasticity in terms of positions and forces of nodes in $\mathcal{G}$:

$$[A^{\intercal} g(|AX|)A]X = B. \tag{5}$$

The application of boundary conditions to system (5) requires a separation of the nodal coordinate directions into two groups: directions with prescribed Neumann condition – a force component, which may be zero (free boundary), and directions with prescribed Dirichlet condition – a new coordinate value which also may be zero (fixed boundary). This separation can be represented by the following expressions for nodal positions and forces, and a correspondingly re-arranged incidence matrix

$$X = \begin{bmatrix} X_1 \\ X_2 \\ \vdots \\ X_p \\ X_{p+1} \\ X_{p+2} \\ \vdots \\ X_{p+q} \end{bmatrix} \in \mathbb{R}^{n\times 3}, \quad B = \begin{bmatrix} B_1 \\ B_2 \\ \vdots \\ B_p \\ B_{p+1} \\ B_{p+2} \\ \vdots \\ B_{p+q} \end{bmatrix} \in \mathbb{R}^{n\times 3},$$

with X_{p+q}, B_{p+q} we denote X_n, B_n respectively. Where

$$\begin{bmatrix} X_1 \\ X_2 \\ \vdots \\ X_p \end{bmatrix} \in \mathbb{R}^{p\times 3}, \quad \text{and} \quad \begin{bmatrix} B_{p+1} \\ B_{p+2} \\ \vdots \\ B_n \end{bmatrix} \in \mathbb{R}^{q\times 3},$$

are vectors of the unknown coordinates and the known corresponding forces, and

$$\begin{bmatrix} X_{p+1} \\ X_{p+2} \\ \vdots \\ X_{p+q} \end{bmatrix} \in \mathbb{R}^{q\times 3}, \quad \begin{bmatrix} B_1 \\ B_2 \\ \vdots \\ B_p \end{bmatrix} \in \mathbb{R}^{p\times 3},$$

are vectors of the known coordinates and the unknown corresponding forces.

3 Main Results

System (5) is a non-linear system. This is because of the diagonal matrix $g(|AX|)$ defined in (1). We provide the following theorem:

Theorem 3.1. Consider the non-linear system (5). Then an effective linearization of the system is given by

$$\tilde{A}X = B. \tag{6}$$

Where $\tilde{A} = A^{\intercal}\tilde{K}A$ with $\tilde{K} = \mathrm{diag}[\tilde{K_i}]_{1\leq i\leq m}$ and

- For $a_i \leq r_i \leq b_i$, $\hat{a}_j \leq \hat{r}_j \leq \hat{b}_j$:

$$\tilde{K_i} = \frac{(a_i+b_i)l_i + \big(2l_i + \sum_{j=1}^{\hat{m}}\big(\frac{\hat{a}_j}{2b_i} + \frac{\hat{b}_j}{2a_i}\big)\hat{l}_j\big)|E_i| + \sum_{j=1}^{\hat{m}}\big(\frac{a_i\hat{a}_j}{2b_i} + \frac{b_i\hat{b}_j}{2a_i}\big)\hat{l}_j}{2(a_i+|E_i|)(b_i+|E_i|)}$$

- For $b_i \leq r_i \leq 0$, $\hat{b}_j \leq \hat{r}_j \leq 0$:

$$\tilde{K_i} = \frac{|F_i|}{|Y_i|} \cong \frac{1}{2b_i}\big[l_i(1 - \frac{|E_i|}{b_i+|E_i|}) + \frac{1}{|E_i|}\sum_{j=1}^{\hat{m}}\hat{l}_j\hat{b}_j\big]$$

- For $0 \leq r_i \leq c_i$, $0 \leq \hat{r}_j \leq \hat{c}_j$:

$$\tilde{K_i} \cong \frac{1}{2c_i}\big[k_i(1 - \frac{|E_i|}{c_i+|E_i|}) + \frac{1}{|E_i|}\sum_{j=1}^{\hat{m}}\hat{k}_j\hat{c}_j\big].$$

- For $c_i \leq r_i \leq d_i$, $\hat{c}_j \leq \hat{r}_j \leq \hat{d}_j$:

$$\tilde{K_i} \cong \frac{(c_i+d_i)k_i + \big(2k_i + \sum_{j=1}^{\hat{m}}\big(\frac{\hat{c}_j}{2d_i} + \frac{\hat{d}_j}{2c_i}\big)\hat{k}_j\big)|E_i| + \sum_{j=1}^{\hat{m}}\big(\frac{c_i\hat{c}_j}{2d_i} + \frac{d_i\hat{d}_j}{2c_i}\big)\hat{k}_j}{2(c_i+|E_i|)(d_i+|E_i|)}.$$

Where $r_i = |Y_i| - |E_i|$, $\hat{r}_j = |\hat{Y}_j| - |\hat{E}_j|$. Let

$$\tilde{A} = \begin{bmatrix} \tilde{A}_{11} & \tilde{A}_{12} \\ \tilde{A}_{21} & \tilde{A}_{22} \end{bmatrix}.$$

Where $\tilde{A}_{11} \in \mathbb{R}^{p\times p}, \tilde{A}_{12} \in \mathbb{R}^{p\times q}, \tilde{A}_{21} \in \mathbb{R}^{q\times q}, \tilde{A}_{22} \in \mathbb{R}^{q\times q}$. Then system (11) can be divided into the following subsystems

$$\tilde{A}_{11}\begin{bmatrix} X_1 \\ X_2 \\ \vdots \\ X_p \end{bmatrix} = \begin{bmatrix} B_1 \\ B_2 \\ \vdots \\ B_p \end{bmatrix} - \tilde{A}_{12}\begin{bmatrix} X_{p+1} \\ X_{p+2} \\ \vdots \\ X_{p+q} \end{bmatrix} \tag{7}$$

and

$$\begin{bmatrix} B_{p+1} \\ B_{p+2} \\ \vdots \\ B_n \end{bmatrix} = \tilde{A}_{21}\begin{bmatrix} X_1 \\ X_2 \\ \vdots \\ X_p \end{bmatrix} + \tilde{A}_{22}\begin{bmatrix} X_{p+1} \\ X_{p+2} \\ \vdots \\ X_{p+q} \end{bmatrix}. \tag{8}$$

From the above systems only (7) has to be solved. Then $\begin{bmatrix} X_1 \\ X_2 \\ \vdots \\ X_p \end{bmatrix}$ can be replaced in (8) and $\begin{bmatrix} B_{p+1} \\ B_{p+2} \\ \vdots \\ B_n \end{bmatrix}$ is easily computed.

Proof. We consider (5) and will seek optimal bounds for $\frac{|F_i|}{|Y_i|}$, $\forall i = 1, 2, ..., m$.

For $a_i \le r_i \le b_i$, $\hat{a}_j \le \hat{r}_j \le \hat{b}_j$ and (3) we have

$$|F_i| = l_i + \frac{1}{2(|Y_i| - |E_i|)} \sum_{j=1}^{\hat{m}} \big[\hat{l}_j \big(|\hat{Y}_j| - |\hat{E}_j|\big)\big], \quad l_i, \hat{l}_j < 0,$$

From Fig. 1 we have that

$$\hat{a}_j \le |\hat{Y}_j| - |\hat{E}_j| \le \hat{b}_j,$$

or, equivalently,

$$\hat{a}_j \hat{l}_j \ge \hat{r}_j \hat{l}_j \ge \hat{b}_j \hat{l}_j,$$

or, equivalently,

$$\frac{1}{2b_i} \sum_{j=1}^{\hat{m}} \hat{a}_j \hat{l}_j \le \frac{1}{2r_i} \sum_{j=1}^{\hat{m}} \hat{r}_j \hat{l}_j \le \frac{1}{2a_i} \sum_{j=1}^{\hat{m}} \hat{b}_j \hat{l}_j,$$

or, equivalently,

$$l_i + \frac{1}{2b_i} \sum_{j=1}^{\hat{m}} \hat{a}_j \hat{l}_j \le |F_i| \le l_i + \frac{1}{2a_i} \sum_{j=1}^{\hat{m}} \hat{b}_j \hat{l}_j,$$

and consequently

$$\frac{l_i + \frac{1}{2b_i} \sum_{j=1}^{\hat{m}} \hat{a}_j \hat{l}_j}{b_i + |E_i|} \le \frac{|F_i|}{|Y_i|} \le \frac{l_i + \frac{1}{2a_i} \sum_{j=1}^{\hat{m}} \hat{b}_j \hat{l}_j}{a_i + |E_i|}.$$

Hence

$$\frac{|F_i|}{|Y_i|} \cong \frac{(a_i + b_i) l_i + \big(2l_i + \sum_{j=1}^{\hat{m}} \big(\frac{\hat{a}_j}{2b_i} + \frac{\hat{b}_j}{2a_i}\big)\hat{l}_j\big)|E_i| + \sum_{j=1}^{\hat{m}} \big(\frac{a_i \hat{a}_j}{2b_i} + \frac{b_i \hat{b}_j}{2a_i}\big)\hat{l}_j}{2(a_i + |E_i|)(b_i + |E_i|)}. \tag{9}$$

For $b_i \le r_i \le 0$, $\hat{b}_j \le \hat{r}_j \le 0$ we have

$$|F_i| = \frac{l_i}{b_i}(|Y_i| - |E_i|) + \frac{1}{2(|Y_i| - |E_i|)} \sum_{j=1}^{\hat{m}} \big[\frac{\hat{l}_j}{\hat{b}_j} \big(|\hat{Y}_j| - |\hat{E}_j|\big)^2\big], \quad l_i, \hat{l}_j < 0,$$

or, equivalently,

$$\frac{|F_i|}{|Y_i|} = \frac{l_i}{b_i}(1 - \frac{|E_i|}{|Y_i|}) + \frac{1}{2|Y_i|(|Y_i| - |E_i|)} \sum_{j=1}^{\hat{m}} [\frac{\hat{l}_j}{\hat{b}_j}\big(|\hat{Y}_j| - |\hat{E}_j|\big)^2], \quad i = 1, 2, ..., m.$$

From Fig. 1 we have that

$$\hat{b}_j \leq |\hat{Y}_j| - |\hat{E}_j| \leq 0,$$

or, equivalently,

$$0 \leq \sum_{j=1}^{\hat{m}} \frac{\hat{l}_j}{\hat{b}_j} \hat{r}_j^2 \leq \sum_{j=1}^{\hat{m}} \hat{l}_j \hat{b}_j,$$

or, equivalently,

$$\frac{1}{2|E_i|r_i} \sum_{j=1}^{\hat{m}} \hat{l}_j \hat{b}_j \leq \frac{1}{2|Y_i|r_i} \sum_{j=1}^{\hat{m}} \frac{\hat{l}_j}{\hat{b}_j} \hat{r}_j^2 \leq 0,$$

or, equivalently,

$$\frac{l_i}{b_i}(1 - \frac{|E_i|}{|Y_i|}) + \frac{1}{2|E_i|r_i} \sum_{j=1}^{\hat{m}} \hat{l}_j \hat{b}_j \leq \frac{|F_i|}{|Y_i|} \leq \frac{l_i}{b_i}(1 - \frac{|E_i|}{|Y_i|}),$$

or, equivalently,

$$\frac{l_i}{b_i}(1 - \frac{|E_i|}{b_i + |E_i|}) + \frac{1}{2|E_i|r_i} \sum_{j=1}^{\hat{m}} \hat{l}_j \hat{b}_j \leq \frac{|F_i|}{|Y_i|} \leq 0,$$

because

$$1 - \frac{|E_i|}{b_i + |E_i|} \leq 1 - \frac{|E_i|}{|Y_i|} \leq 0.$$

Consequently

$$\frac{|F_i|}{|Y_i|} \cong \frac{1}{2b_i}\big[l_i(1 - \frac{|E_i|}{b_i + |E_i|}) + \frac{1}{|E_i|} \sum_{j=1}^{\hat{m}} \hat{l}_j \hat{b}_j\big]. \tag{10}$$

For $0 \leq r_i \leq c_i$, $0 \leq \hat{r}_j \leq \hat{c}_j$ we have

$$|F_i| = \frac{k_i}{c_i}(|Y_i| - |E_i|) + \frac{1}{2(|Y_i| - |E_i|)} \sum_{j=1}^{\hat{m}} [\frac{\hat{k}_j}{\hat{c}_j}\big(|\hat{Y}_j| - |\hat{E}_j|\big)^2], \quad k_i, \hat{k}_j > 0, \quad i = 1, 2, ..., m.$$

or, equivalently,

$$\frac{|F_i|}{|Y_i|} = \frac{k_i}{c_i}(1 - \frac{|E_i|}{|Y_i|}) + \frac{1}{2|Y_i|(|Y_i| - |E_i|)} \sum_{j=1}^{\hat{m}} [\frac{\hat{k}_j}{\hat{c}_j}\big(|\hat{Y}_j| - |\hat{E}_j|\big)^2], \quad i = 1, 2, ..., m.$$

From Fig. 1 we have that

$$0 \leq |\hat{Y}_j| - |\hat{E}_j| \leq \hat{c}_j,$$

or, equivalently,

$$0 \leq \sum_{j=1}^{\hat{m}} \frac{\hat{k}_j}{\hat{c}_j} \hat{r}_j^2 \leq \sum_{j=1}^{\hat{m}} \hat{k}_j \hat{c}_j,$$

or, equivalently,

$$0 \leq \frac{1}{2|Y_i|r_i} \sum_{j=1}^{\hat{m}} \frac{\hat{k}_j}{\hat{c}_j} \hat{r}_j^2 \leq \frac{1}{2|E_i|r_i} \sum_{j=1}^{\hat{m}} \hat{k}_j \hat{c}_j,$$

or, equivalently,

$$\frac{k_i}{c_i}(1 - \frac{|E_i|}{|Y_i|}) \leq \frac{|F_i|}{|Y_i|} \leq \frac{k_i}{c_i}(1 - \frac{|E_i|}{|Y_i|}) + \frac{1}{2|E_i|r_i} \sum_{j=1}^{\hat{m}} \hat{k}_j \hat{c}_j,$$

or, equivalently,

$$0 \leq \frac{|F_i|}{|Y_i|} \leq \frac{k_i}{c_i}(1 - \frac{|E_i|}{c_i + |E_i|}) + \frac{1}{2|E_i|r_i} \sum_{j=1}^{\hat{m}} \hat{k}_j \hat{c}_j,$$

because

$$0 \leq 1 - \frac{|E_i|}{|Y_i|} \leq 1 - \frac{|E_i|}{c_i + |E_i|}.$$

Consequently

$$\frac{|F_i|}{|Y_i|} \cong \frac{1}{2c_i} \big[k_i(1 - \frac{|E_i|}{c_i + |E_i|}) + \frac{1}{|E_i|} \sum_{j=1}^{\hat{m}} \hat{k}_j \hat{c}_j \big]. \tag{11}$$

For $c_i \leq r_i \leq d_i$, $\hat{c}_j \leq \hat{r}_j \leq \hat{d}_j$ and (3) we have

$$|F_i| = k_i + \frac{1}{2(|Y_i| - |E_i|)} \sum_{j=1}^{\hat{m}} \big[\hat{k}_j \big(|\hat{Y}_j| - |\hat{E}_j| \big) \big], \quad k_i, \hat{k}_j > 0, \quad i = 1, 2, ..., m.$$

From Fig. 1 we have that

$$\hat{c}_j \leq |\hat{Y}_j| - |\hat{E}_j| \leq \hat{d}_j,$$

or, equivalently,

$$\frac{1}{2d_i} \sum_{j=1}^{\hat{m}} \hat{c}_j \hat{k}_j \leq \frac{1}{2r_i} \sum_{j=1}^{\hat{m}} \hat{r}_j \hat{k}_j \leq \frac{1}{2c_i} \sum_{j=1}^{\hat{m}} \hat{d}_j \hat{k}_j,$$

or, equivalently,

$$k_i + \frac{1}{2d_i}\sum_{j=1}^{\hat{m}} \hat{c}_j\hat{k}_j \leq |F_i| \leq k_i + \frac{1}{2c_i}\sum_{j=1}^{\hat{m}} \hat{d}_j\hat{k}_j,$$

and consequently

$$\frac{k_i + \frac{1}{2d_i}\sum_{j=1}^{\hat{m}} \hat{c}_j\hat{k}_j}{d_i + |E_i|} \leq \frac{|F_i|}{|Y_i|} \leq \frac{k_i + \frac{1}{2c_i}\sum_{j=1}^{\hat{m}} \hat{d}_j\hat{k}_j}{c_i + |E_i|},$$

Hence

$$\frac{|F_i|}{|Y_i|} \cong \frac{(c_i+d_i)k_i + \big(2k_i + \sum_{j=1}^{\hat{m}} \big(\frac{\hat{c}_j}{2d_i} + \frac{\hat{d}_j}{2c_i}\big)\hat{k}_j\big)|E_i| + \sum_{j=1}^{\hat{m}} \big(\frac{c_i\hat{c}_j}{2d_i} + \frac{d_i\hat{d}_j}{2c_i}\big)\hat{k}_j}{2(c_i+|E_i|)(d_i+|E_i|)}, \tag{12}$$

System (5) can be written as

$$\begin{bmatrix} \tilde{A}_{11} & \tilde{A}_{12} \\ \tilde{A}_{21} & \tilde{A}_{22} \end{bmatrix} \begin{bmatrix} X_1 \\ X_2 \\ \vdots \\ X_p \\ X_{p+1} \\ X_{p+2} \\ \vdots \\ X_{p+q} \end{bmatrix} = \begin{bmatrix} B_1 \\ B_2 \\ \vdots \\ B_p \\ B_{p+1} \\ B_{p+2} \\ \vdots \\ B_{p+q} \end{bmatrix},$$

or, equivalently,

$$\tilde{A}_{11} \begin{bmatrix} X_1 \\ X_2 \\ \vdots \\ X_p \end{bmatrix} + \tilde{A}_{12} \begin{bmatrix} X_{p+1} \\ X_{p+2} \\ \vdots \\ X_{p+q} \end{bmatrix} = \begin{bmatrix} B_1 \\ B_2 \\ \vdots \\ B_p \end{bmatrix},$$

and

$$\tilde{A}_{21} \begin{bmatrix} X_1 \\ X_2 \\ \vdots \\ X_p \end{bmatrix} + \tilde{A}_{22} \begin{bmatrix} X_{p+1} \\ X_{p+2} \\ \vdots \\ X_{p+q} \end{bmatrix} = \begin{bmatrix} B_{p+1} \\ B_{p+2} \\ \vdots \\ B_n \end{bmatrix}.$$

From the above expressions we get the subsystems (7), (8). The proof is completed. □

Theorem 3.1 presents a solution for the non-linear system (5) by utilizing the linear system (6). This method offers several advantages, including the ability to analyze solutions of non-linear systems involving large matrices at a minimal computational cost, thanks to the linearity of (6). Furthermore, the proposed method proves to be user-friendly for handling non-linear systems not only in the present context but also in various other applications, including electrical networks [18, 19], gas networks [20], and dynamical networks [21, 22, 23].

4 Numerical Example

In this section, we illustrate the main results of the paper through a numerical example. In particular, we consider a system comprising a lattice $\mathcal{G}$ of $n = 6$ nodes with coordinates $N = [N_1\ N_2\ \dots N_6]^\intercal$, which are connected through $m = 12$ edges with vector values $E = [E_1\ E_2\ \dots\ E_{12}]^\intercal$. In addition, the midpoints of the 12 edges of the lattice are also the coordinates $\hat{N} = [\hat{N}_1\ \hat{N}_2\ \dots\ \hat{N}_{12}]^\intercal$ of a second lattice $\hat{\mathcal{G}}$ with $\hat{n} = 12$ nodes. The nodes of the second lattice are connected through $\hat{m} = 36$ edges with vector values $\hat{E} = [\hat{E}_1\ \hat{E}_2\ \dots\ \hat{E}_{36}]^\intercal$. The values of the components of N, E, $\hat{N}$ and $\hat{E}$ are given in Table 1. A three-dimensional representation of the graphs of the two lattices is shown in Fig. 2a, while a two-dimensional representation of the same graphs is given in Fig. 2b.

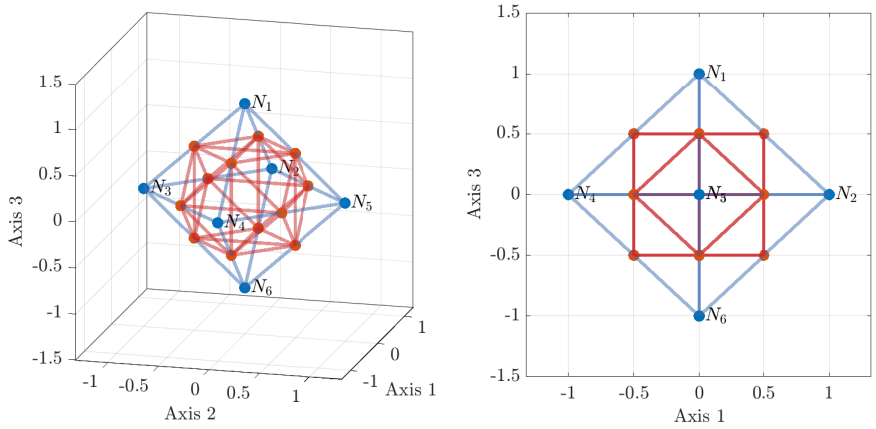

(a) 3D plot.

(b) 2D plot.

Figure 2: Lattice $\mathcal{G}$ and $\hat{\mathcal{G}}$ graphs in initial positions.

The incidence matrix corresponding to $\mathcal{G}$ is:

$$A = \begin{bmatrix} 1 & 0 & 0 & -1 & 0 & 0 \\ 1 & 0 & 0 & 0 & -1 & 0 \\ 1 & -1 & 0 & 0 & 0 & 0 \\ 1 & 0 & -1 & 0 & 0 & 0 \\ 0 & 0 & 1 & -1 & 0 & 0 \\ 0 & 0 & 0 & 1 & -1 & 0 \\ 0 & -1 & 0 & 0 & 1 & 0 \\ 0 & 1 & -1 & 0 & 0 & 0 \\ 0 & 0 & 0 & -1 & 0 & 1 \\ 0 & 0 & 0 & 0 & -1 & 1 \\ 0 & -1 & 0 & 0 & 0 & 1 \\ 0 & 0 & -1 & 0 & 0 & 1 \end{bmatrix},$$

while the incidence matrix corresponding to $\hat{\mathcal{G}}$ is:

$$\hat{A} = \begin{bmatrix}
1 & -1 & 0 & 0 & 0 & 0 & 0 & 0 & 0 & 0 & 0 & 0 \\
1 & 0 & 0 & -1 & 0 & 0 & 0 & 0 & 0 & 0 & 0 & 0 \\
1 & 0 & 0 & 0 & -1 & 0 & 0 & 0 & 0 & 0 & 0 & 0 \\
1 & 0 & 0 & 0 & 0 & -1 & 0 & 0 & 0 & 0 & 0 & 0 \\
0 & 1 & -1 & 0 & 0 & 0 & 0 & 0 & 0 & 0 & 0 & 0 \\
0 & 1 & 0 & 0 & 0 & -1 & 0 & 0 & 0 & 0 & 0 & 0 \\
0 & 1 & 0 & 0 & 0 & 0 & -1 & 0 & 0 & 0 & 0 & 0 \\
0 & 0 & 1 & -1 & 0 & 0 & 0 & 0 & 0 & 0 & 0 & 0 \\
0 & 0 & 0 & 1 & -1 & 0 & 0 & 0 & 0 & 0 & 0 & 0 \\
0 & 0 & 0 & 1 & 0 & 0 & 0 & -1 & 0 & 0 & 0 & 0 \\
0 & 0 & 1 & 0 & 0 & 0 & -1 & 0 & 0 & 0 & 0 & 0 \\
0 & 0 & 1 & 0 & 0 & 0 & 0 & -1 & 0 & 0 & 0 & 0 \\
0 & 1 & 0 & -1 & 0 & 0 & 0 & 0 & 0 & 0 & 0 & 0 \\
1 & 0 & 0 & 0 & 0 & 0 & 0 & 0 & -1 & 0 & 0 & 0 \\
0 & 1 & 0 & 0 & 0 & 0 & 0 & 0 & 0 & -1 & 0 & 0 \\
1 & 0 & -1 & 0 & 0 & 0 & 0 & 0 & 0 & 0 & 0 & 0 \\
0 & 0 & 0 & 0 & 0 & 0 & 0 & 0 & 1 & 0 & 0 & -1 \\
0 & 0 & 0 & 0 & 0 & 0 & 0 & 0 & 0 & 1 & -1 & 0 \\
0 & 0 & 0 & 0 & 0 & 0 & 0 & 0 & 0 & 0 & 1 & -1 \\
0 & 0 & 0 & 0 & 0 & 1 & 0 & 0 & -1 & 0 & 0 & 0 \\
0 & 0 & 0 & 0 & 0 & 1 & 0 & 0 & 0 & -1 & 0 & 0 \\
0 & 0 & 0 & 0 & 0 & 0 & 1 & 0 & 0 & 0 & -1 & 0 \\
0 & 0 & 0 & 0 & 0 & 0 & 1 & 0 & 0 & -1 & 0 & 0 \\
0 & 0 & 0 & 0 & 1 & 0 & 0 & 0 & -1 & 0 & 0 & 0 \\
0 & 0 & 0 & 0 & 1 & 0 & 0 & 0 & 0 & 0 & 0 & -1 \\
0 & 0 & 0 & 0 & 0 & 0 & 0 & 1 & 0 & 0 & -1 & 0 \\
0 & 0 & 0 & 0 & 0 & 0 & 0 & 1 & 0 & 0 & 0 & -1 \\
0 & 0 & 0 & 0 & 0 & 0 & 0 & 0 & 1 & -1 & 0 & 0 \\
0 & 0 & 1 & 0 & 0 & 0 & 0 & 0 & 0 & 0 & -1 & 0 \\
0 & 0 & 0 & 1 & 0 & 0 & 0 & 0 & 0 & 0 & 0 & -1 \\
0 & 0 & 0 & 0 & 1 & -1 & 0 & 0 & 0 & 0 & 0 & 0 \\
0 & 0 & 0 & 0 & 1 & 0 & 0 & -1 & 0 & 0 & 0 & 0 \\
0 & 0 & 0 & 0 & 0 & 1 & -1 & 0 & 0 & 0 & 0 & 0 \\
0 & 0 & 0 & 0 & 0 & 0 & 1 & -1 & 0 & 0 & 0 & 0 \\
0 & 0 & 0 & 0 & 0 & 0 & 0 & 0 & 1 & 0 & -1 & 0 \\
0 & 0 & 0 & 0 & 0 & 0 & 0 & 0 & 0 & 1 & 0 & -1
\end{bmatrix},$$

We now assume the application of an external force to the examined structure. As a result, the geometry of the structure is deformed, and the nodes of $\mathcal{G}$ and $\hat{\mathcal{G}}$ have new coordinates X and $\hat{X}$, respectively. Moreover, the new values of the edge vectors of $\mathcal{G}$ and $\hat{\mathcal{G}}$ of the deformed structure are given by Y and $\hat{Y}$, respectively. Then, the length change of the i-th edge of $\mathcal{G}$ due to the applied force is given by $r_i = |Y_i| - |E_i|$, while the length change of the j-th edge of $\hat{\mathcal{G}}$ is given by $\hat{r}_j = |\hat{Y}_j| - |\hat{E}_j|$. In the remainder of this example we consider the following cases:

i	N_i	$\hat{N}_i$	E_i	$\lvert E_i\rvert$	$\hat{E}_i$	$\lvert\hat{E}_i\rvert$
1	(0, 0,1)	(-0.5,0,0.5)	(1,0,1)	$\sqrt{2}$	(-0.5,-0.5,0)	$1/\sqrt{2}$
2	(1,0,0)	(0,0.5,0.5)	(0,-1,1)	$\sqrt{2}$	(-0.5,0.5,0)	$1/\sqrt{2}$
3	(0,-1,0)	(0.5,0,0.5)	(-1,0,1)	$\sqrt{2}$	(0.5,0.5,0)	$1/\sqrt{2}$
4	(-1,0,0)	(0,-0.5,0.5)	(0,1,1)	$\sqrt{2}$	(0.5,-0.5,0)	$1/\sqrt{2}$
5	(0,1,0)	(-0.5,-0.5,0)	(1,-1,0)	$\sqrt{2}$	(0,0.5,0.5)	$1/\sqrt{2}$
6	(0,0,-1)	(-0.5,0.5,0)	(-1,-1,0)	$\sqrt{2}$	(0,-0.5,0.5)	$1/\sqrt{2}$
7		(0.5,0.5,0)	(-1,1,0)	$\sqrt{2}$	(0.5,0,0.5)	$1/\sqrt{2}$
8		(0.5,-0.5,0)	(1,1,0)	$\sqrt{2}$	(-0.5,0,0.5)	$1/\sqrt{2}$
9		(-0.5,0,-0.5)	(1,0,-1)	$\sqrt{2}$	(0,-0.5,0.5)	$1/\sqrt{2}$
10		(0,0.5,-0.5)	(0,-1,-1)	$\sqrt{2}$	(0,0.5,0.5)	$1/\sqrt{2}$
11		(0.5,0,-0.5)	(-1,0,-1)	$\sqrt{2}$	(-0.5,0,0.5)	$1/\sqrt{2}$
12		(0,-0.5,-0.5)	(0,1,-1)	$\sqrt{2}$	(0.5,0,0.5)	$1/\sqrt{2}$
13					(0,-1,0)	1
14					(-1,0,0)	1
15					(0,1,0)	1
16					(1,0,0)	1
17					(-0.5,0,0.5)	$1/\sqrt{2}$
18					(0,-0.5,0.5)	$1/\sqrt{2}$
19					(0,0.5,0.5)	$1/\sqrt{2}$
20					(-0.5,0,0.5)	$1/\sqrt{2}$
21					(0.5,0,0.5)	$1/\sqrt{2}$
22					(0,0.5,0.5)	$1/\sqrt{2}$
23					(0,-0.5,0.5)	$1/\sqrt{2}$
24					(0.5,0,0.5)	$1/\sqrt{2}$
25					(-0.5,-0.5,0)	$1/\sqrt{2}$
26					(-0.5,0.5,0)	$1/\sqrt{2}$
27					(0.5,0.5,0)	$1/\sqrt{2}$
28					(0.5,-0.5,0)	$1/\sqrt{2}$
29					(-1,0,0)	1
30					(0,1,0)	1
31					(-1,0,0)	1
32					(0,1,0)	1
33					(0,0,1)	1
34					(0,0,1)	1
35					(0,0,1)	1
36					(0,0,1)	1

Table 1: Initial nodes, edges, and edge lengths.

- $0 \le r_i \le c_i$, $0 \le \hat{r}_j \le \hat{c}_j$, and
- $c_i \le r_i \le d_i$, $\hat{c}_j \le \hat{r}_j \le \hat{d}_j$,

where the values of c_i, d_i, $\hat{c}_j$ and $\hat{d}_j$ are given in Table 2.

First, for $0 \le r_i \le c_i$, $0 \le \hat{r}_j \le \hat{c}_j$, we find from Theorem 3.1 that $\tilde{K}_i = 6.44 \cdot 10^{-4}$, $i = 1, 2, \ldots, m$, where the values of k_i and $\hat{k}_j$ are given in Table 2.

i	c_i	d_i	$\hat{c}_i$	$\hat{d}_i$	$k_i \times 10^4$	$\hat{k}_i \times 10^4$	B_i
1	0.2121	7.0711	0.1061	3.5355	$\sqrt{2}$	$1/\sqrt{2}$	(0,0,0.1586)
2	0.2121	7.0711	0.1061	3.5355	$\sqrt{2}$	$1/\sqrt{2}$	(0.1760,0,0)
3	0.2121	7.0711	0.1061	3.5355	$\sqrt{2}$	$1/\sqrt{2}$	(0,-0.1954,0)
4	0.2121	7.0711	0.1061	3.5355	$\sqrt{2}$	$1/\sqrt{2}$	(-0.2169,0,0)
5	0.2121	7.0711	0.1061	3.5355	$\sqrt{2}$	$1/\sqrt{2}$	(0,0.2407,0)
6	0.2121	7.0711	0.1061	3.5355	$\sqrt{2}$	$1/\sqrt{2}$	
7	0.2121	7.0711	0.1061	3.5355	$\sqrt{2}$	$1/\sqrt{2}$	
8	0.2121	7.0711	0.1061	3.5355	$\sqrt{2}$	$1/\sqrt{2}$	
9	0.2121	7.0711	0.1061	3.5355	$\sqrt{2}$	$1/\sqrt{2}$	
10	0.2121	7.0711	0.1061	3.5355	$\sqrt{2}$	$1/\sqrt{2}$	
11	0.2121	7.0711	0.1061	3.5355	$\sqrt{2}$	$1/\sqrt{2}$	
12	0.2121	7.0711	0.1061	3.5355	$\sqrt{2}$	$1/\sqrt{2}$	
13			0.1500	5		1	
14			0.1500	5		1	
15			0.1500	5		1	
16			0.1500	5		1	
17			0.1061	3.5355		$1/\sqrt{2}$	
18			0.1061	3.5355		$1/\sqrt{2}$	
19			0.1061	3.5355		$1/\sqrt{2}$	
20			0.1061	3.5355		$1/\sqrt{2}$	
21			0.1061	3.5355		$1/\sqrt{2}$	
22			0.1061	3.5355		$1/\sqrt{2}$	
23			0.1061	3.5355		$1/\sqrt{2}$	
24			0.1061	3.5355		$1/\sqrt{2}$	
25			0.1061	3.5355		$1/\sqrt{2}$	
26			0.1061	3.5355		$1/\sqrt{2}$	
27			0.1061	3.5355		$1/\sqrt{2}$	
28			0.1061	3.5355		$1/\sqrt{2}$	
29			0.15	5		1	
30			0.15	5		1	
31			0.15	5		1	
32			0.15	5		1	
33			0.15	5		1	
34			0.15	5		1	
35			0.15	5		1	
36			0.15	5		1	

Table 2: Given forces on nodes and material properties.

Then, we have $\tilde{A} = A^\intercal \tilde{K} A$. Matrix $\tilde{A}$ can be written as:

$$\tilde{A} = \begin{bmatrix} \tilde{A}_{11} & \tilde{A}_{12} \\ \tilde{A}_{21} & \tilde{A}_{22} \end{bmatrix}, \tag{13}$$

where

$$\tilde{A}_{11} = \begin{bmatrix} 0.0026 & -0.0006 & -0.0006 & -0.0006 & -0.0006 \\ -0.0006 & 0.0026 & -0.0006 & 0 & -0.0006 \\ -0.0006 & -0.0006 & 0.0026 & -0.0006 & 0 \\ -0.0006 & 0 & -0.0006 & 0.0026 & -0.0006 \\ -0.0006 & -0.0006 & 0 & -0.0006 & 0.0026 \end{bmatrix},$$

$$\tilde{A}_{21} = \tilde{A}_{12}^{\intercal} = \begin{bmatrix} 0 & -0.0006 & -0.0006 & -0.0006 & -0.0006 \end{bmatrix}, \quad \tilde{A}_{22} = 0.0026\,.$$

Given the values of B_i, $i = 1, 2, \ldots, 5$, in Table 2, and that $X_6 = N_6 = (0, 0, -1)$, we can compute the final positions X of the nodes of $\mathcal{G}$ through the solution of (7):

$$X = \begin{bmatrix} -15.89 & 17.59 & 123.2 \\ 57.77 & 14.66 & 61.6) \\ -13.24 & -64.16 & 61.6 \\ -94.83 & 14.66 & 61.6 \\ -13.24 & 105.22 & 61.6 \\ 0 & 0 & -1 \end{bmatrix}.$$

Moreover, as a byproduct, we find from (8) that $B_6 = (0.04, -0.05, -0.16)$.

Finally, the new positions $\hat{X}$ of the nodes of $\hat{\mathcal{G}}$ are computed through the relationship $\hat{X} = SX$, where for this example:

$$S = \begin{bmatrix} 0.5 & 0 & 0 & 0.5 & 0 & 0 \\ 0.5 & 0 & 0 & 0 & 0.5 & 0 \\ 0.5 & 0.5 & 0 & 0 & 0 & 0 \\ 0.5 & 0 & 0.5 & 0 & 0 & 0 \\ 0 & 0 & 0.5 & 0.5 & 0 & 0 \\ 0 & 0 & 0 & 0.5 & 0.5 & 0 \\ 0 & 0.5 & 0 & 0 & 0.5 & 0 \\ 0 & 0.5 & 0.5 & 0 & 0 & 0 \\ 0 & 0 & 0 & 0.5 & 0 & 0.5 \\ 0 & 0 & 0 & 0 & 0.5 & 0.5 \\ 0 & 0.5 & 0 & 0 & 0 & 0.5 \\ 0 & 0 & 0.5 & 0 & 0 & 0.5 \end{bmatrix}. \tag{14}$$

We find:

$$\hat{X} = \begin{bmatrix} -55.36 & 16.12 & 92.40 \\ -14.56 & 61.41 & 92.40 \\ 20.94 & 16.13 & 92.40 \\ -14.56 & -23.28 & 92.40 \\ -54.03 & -24.75 & 61.60 \\ -54.03 & 59.94 & 61.60 \\ 22.27 & 59.94 & 61.60 \\ 22.27 & -24.75 & 61.60 \\ -47.42 & 7.33 & 30.30 \\ -6.62 & 52.61 & 30.30 \\ 28.88 & 7.33 & 30.30 \\ -6.62 & -32.08 & 30.30 \end{bmatrix}.$$

A three-dimensional representation of the graphs of the two lattices in their final positions is depicted in Fig. 3a, while a two-dimensional plot of the same graphs is depicted in Fig. 3b.

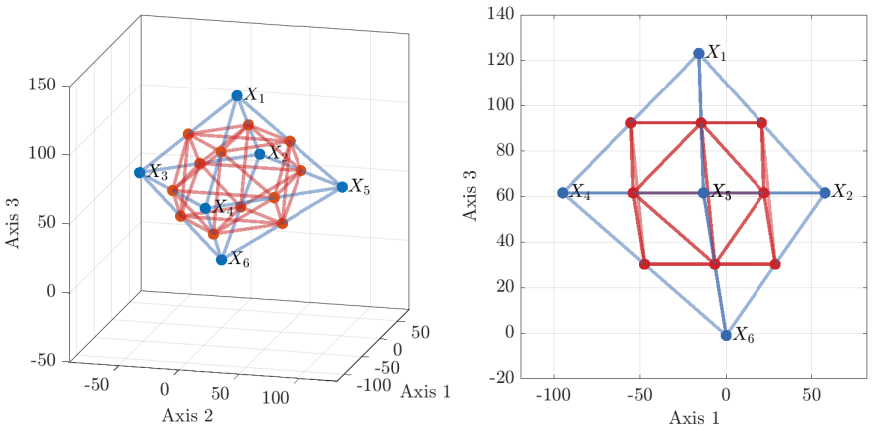

(a) 3D plot.

(b) 2D plot.

Figure 3: Lattice $\mathcal{G}$ and $\hat{\mathcal{G}}$ graphs in final positions ($0 \leq r_i \leq c_i$, $0 \leq \hat{r}_j \leq \hat{c}_j$).

Second, for $c_i \leq r_i \leq d_i$, $\hat{c}_j \leq \hat{r}_j \leq \hat{d}_j$, from Theorem 3.1 we get that $\tilde{K}_i = 0.0088$, $i = 1, 2, \ldots, m$. Then, then $\tilde{A}$ is given by $\tilde{A} = A^\intercal \tilde{K} A$ and can be written in the form of (13), where in this case:

$$\tilde{A}_{11} = \begin{bmatrix} 0.035 & -0.0088 & -0.0088 & -0.0088 & -0.0088 \\ -0.0088 & 0.035 & -0.0088 & 0 & -0.0088 \\ -0.0088 & -0.0088 & 0.035 & -0.0088 & 0 \\ -0.0088 & 0 & -0.0088 & 0.035 & -0.0088 \\ -0.0088 & -0.0088 & 0 & -0.0088 & 0.035 \end{bmatrix},$$

$$\tilde{A}_{21} = \tilde{A}_{12}^\intercal = \begin{bmatrix} 0 & -0.0088 & -0.0088 & -0.0088 & -0.0088 \end{bmatrix}, \quad \tilde{A}_{22} = 0.035\,.$$

The final positions X of the nodes of $\mathcal{G}$ are computed through the solution of (7):

$$X = \begin{bmatrix} -1.17 & 1.29 & 9.06 \\ 4.25 & 1.08 & 4.52 \\ -0.97 & -4.72 & 4.52 \\ -6.98 & 1.08 & 4.52 \\ -0.97 & 7.74 & 4.52 \\ 0 & 0 & -1 \end{bmatrix}.$$

Moreover, from (8), we get that $B_6 = (0.04, -0.05, -0.19)$.

Finally, the new positions $\hat{X}$ of the nodes of $\hat{\mathcal{G}}$ can be found through the

relationship $\hat{X} = SX$, where S is given by (14). We find:

$$\hat{X} = \begin{bmatrix} -4.07 & 1.18 & 6.79 \\ -1.07 & 4.52 & 6.79 \\ 1.54 & 1.19 & 6.79 \\ -1.07 & -1.71 & 6.79 \\ -3.97 & -1.82 & 4.52 \\ -3.97 & 4.41 & 4.52 \\ 1.64 & 4.41 & 4.52 \\ 1.64 & -1.82 & 4.52 \\ -3.49 & 0.54 & 1.76 \\ -0.49 & 3.87 & 1.76 \\ 2.12 & 0.54 & 1.76 \\ -0.49 & -2.36 & 1.76 \end{bmatrix}.$$

Finally, a three-dimensional representation of the graphs of the two lattices in their final positions for the case $c_i \leq r_i \leq d_i$, $\hat{c}_j \leq \hat{r}_j \leq \hat{d}_j$ is presented in Fig. 4a, while a two-dimensional plot of the same graphs is presented in Fig. 4b.

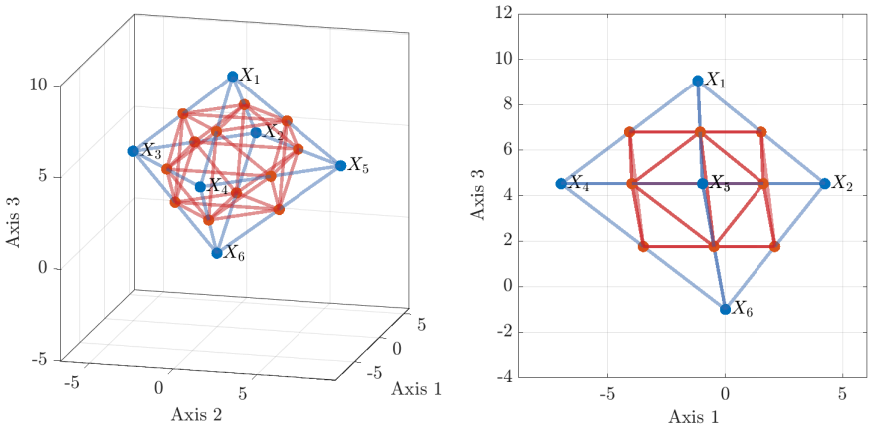

(a) 3D plot.

(b) 2D plot.

Figure 4: Lattice $\mathcal{G}$ and $\hat{\mathcal{G}}$ graphs in final positions ($c_i \leq r_i \leq d_i$, $\hat{c}_j \leq \hat{r}_j \leq \hat{d}_j$).

The graphs shown in this section have been generated with an ad hoc Matlab script, which is available for download at [24].

Conclusions

In this article we proposed a mathematical model of elasticity and plasticity by using DEC and a force-based approach, where the discrete structure of materials is represented by two graphs. By making the kinematics of one of the graphs induced by the kinematics of the other, we derived the governing equations

of elasticity and plasticity, where the deformations of both graphs contribute energy to the system, but the reaction of the system is only via forces in the edges of latter graph. This provides a single non-linear system of governing equations, for which we offered linearization, computational implementation, and a simple demonstration of the model at work.

The model requires extensive testing with larger lattices to compare with experimentally measured elastic behaviour of various materials, which is a subject of ongoing work. We anticipate that the model can be used for atomic-scale simulations as an alternative to the currently used in molecular dynamics interactions based on empirical pair and cohesive potentials. The reason for our expectation is that the inclusion of the complementary lattice in our model could be a suitable replacement to the cohesive potentials including those with angular dependencies.

Acknowledgments

This work was supported by Sustainable Energy Authority of Ireland (SEAI), by funding Ioannis Dassios and Federico Milano via grant no. RDD/00681; by the Swiss National Science Foundation, by funding Georgios Tzounas under NCCR Automation (grant no. 51NF40 18054); and by the Engineering and Physical Sciences Research Coincil, UK, by funding Andrey Jivkov via grant EP/N026136/1.

References

[1] D.V. Griffiths, G.G.W. Mustoe. Modelling of elastic continua using a grillage of structural elements based on discrete element concepts. International Journal for Numerical Methods in Engineering 50 (2001) 1759-1775.

[2] G. Cusatis, Z.P. Bazant, L. Cedolin. Confinement-shear lattice CSL model for fracture propagation in concrete. Computer Methods in Applied Mechanics and Engineering 195 (2006) 7154-7171.

[3] K. Park, G.H. Paulino. Cohesive zone models: A critical review of traction-separation relationships across fracture surfaces. Applied Mechanics Reviews 64 (2011) 061002.

[4] J. Mazars. A description of micro- and macroscale damage of concrete structures. Engineering Fracture Mechanics 25 (1986) 729-737.

[5] J. Lubliner, J. Oliver, S. Oller, E. Onate. A plastic-damage model for concrete. International Journal of Solids and Structures 25 (1989) 299-326.

[6] L. Xue. Damage accumulation and fracture initiation in uncracked ductile solids subject to triaxial loading. International Journal of Solids and Structures 44 (2007) 5163-5181.

[7] B.L. Karihaloo,P.F. Shao, Q.Z. Xiao. Lattice modelling of the failure of particle composites. Engineering Fracture Mechanics 70 (2003) 2385-2406.

[8] A.P. Jivkov, J.R. Yates. Elastic behaviour of a regular lattice for meso-scale modelling of solids. International Journal of Solids and Structures 49 (2012) 3089-3099.

[9] M. Zhang, C.N. Morrison, A.P. Jivkov. A meso-scale site-bond model for elasticity: Theory and calibration. Materials Research Innovations 18 (2014) S2-982-986.

[10] Y. Wang, P. Mora. Macroscopic elastic properties of regular lattices. Journal of the Mechanics and Physics of Solids 56 (2008) 3459-3474.

[11] L.J. Grady, J.R. Polimeni. Discrete Calculus: Applied Analysis on Graphs for Computational Science. Springer, London, 2010.

[12] A.N. Hirani. Discrete exterior calculus. Ph.D. thesis, California Institute of Technology, USA, 2003.

[13] P.D. Boom, A. Seepujak, O. Kosmas, L. Margetts, A.P. Jivkov. Parallelized discrete exterior calculus for three-dimensional elliptic problems. Computer Physics Communications 279 (2022) 108456.

[14] K. Berbatov, P.D. Boom, A.L. Hazel, A.P. Jivkov. Diffusion in multi-dimensional solids using Forman's combinatorial differential forms. Applied Mathematical Modelling 110 (2022) 172–192.

[15] P.D. Boom, O. Kosmas, L. Margetts, A.P. Jivkov. A geometric formulation of linear elasticity based on Discrete Exterior Calculus. International Journal of Solids and Structures 236-237 (2022) 111345.

[16] I. Dassios, A.P. Jivkov, A. Abu-Muharib, P. James. A mathematical model for plasticity and damage: A discrete calculus formulation. Journal of Computational and Applied Mathematics 312 (2017) 27-38.

[17] I. Dassios, A.P. Jivkov, G. O' Keeffe. A mathematical model for elasticity using calculus on discrete manifolds. Mathematical Methods in the Applied Sciences 41 (2018) 9057-9070.

[18] I. Dassios, P. Cuffe, A. Keane. Calculating Nodal Voltages Using the Admittance Matrix Spectrum of an Electrical Network. Mathematics 7(1) (2019) 106.

[19] I. Dassios, P. Cuffe, A. Keane. Visualizing Voltage Security Using The Unity Row Summation and Real Valued Properties of the F_{LG} Matrix. Electric Power Systems Research 140 (2016) 611-618.

[20] A. Ekhtiari, I. Dassios, M. Liu, E. Syron. A Novel Approach to Model a Gas Network. Applied Sciences 9(6) (2019) 1024.

[21] I. Dassios, G. Tzounas, F. Milano. A bounded dynamical network of curves and the stability of its steady states. Mathematical Methods in the Applied Sciences (2023). https://doi.org/10.1002/mma.9390

[22] I. Dassios. Stability of Bounded Dynamical Networks with Symmetry. Symmetry 10(4) (2018) 12.

[23] I. Dassios. Stability of basic steady states of networks in bounded domains. Computers & Mathematics with Applications 70(9) (2015) 2177-2196.

[24] I. Dassios, G. Tzounas, A. Jivkov, F. Milano. MATLAB script for example in 2023 paper: A Discrete Model on Force-Based Elasticity and Plasticity. Zenodo (2023). https://doi.org/10.5281/zenodo.8185531